

# Quantum network communication: a discrete-time quantum-walk approach

Yuguang YANG<sup>1,2\*</sup>, Jiajie YANG<sup>1</sup>, Yihua ZHOU<sup>1</sup>, Weimin SHI<sup>1</sup>, Xiubo CHEN<sup>3</sup>,  
Jian LI<sup>4</sup> & Huijuan ZUO<sup>5</sup>

<sup>1</sup>Faculty of Information Technology, Beijing University of Technology, Beijing 100124, China;

<sup>2</sup>State Key Laboratory of Information Security (Institute of Information Engineering,  
Chinese Academy of Sciences), Beijing 100093, China;

<sup>3</sup>Information Security Center, State Key Laboratory of Networking and Switching Technology,  
Beijing University of Posts and Telecommunications, Beijing 100876, China;

<sup>4</sup>School of Computer, Beijing University of Posts and Telecommunications, Beijing 100876, China;

<sup>5</sup>College of Mathematics and Information Science, Hebei Normal University, Shijiazhuang 050024, China

Received 9 May 2017/Revised 24 June 2017/Accepted 27 July 2017/Published online 5 January 2018

**Abstract** We study the problem of quantum multi-unicast communication over the butterfly network in a quantum-walk architecture, where multiple arbitrary single-qubit states are transmitted simultaneously between multiple source-sink pairs. Here, by introducing quantum walks, we demonstrate a quantum multi-unicast communication scheme over the butterfly network and the inverted crown network, respectively, where the arbitrary single-qubit states can be efficiently transferred with both the probability and the state fidelity one. The presented result concerns only the butterfly network and the inverted crown network, but our techniques can be applied to a more general graph. It paves a way to combine quantum computation and quantum network communication.

**Keywords** network coding, quantum network coding, quantum walk, state fidelity, butterfly network, inverted crown network

**Citation** Yang Y G, Yang J J, Zhou Y H, et al. Quantum network communication: a discrete-time quantum-walk approach. *Sci China Inf Sci*, 2018, 61(4): 042501, <https://doi.org/10.1007/s11432-017-9190-0>

## 1 Introduction

Network communication was traditionally done by the store-and-forward model, i.e., “routing” in which the received data is simply copied and forwarded without any data processing. Some kinds of network communication [1, 2] have been studied. Zhou et al. [1] designed an efficient near-duplicate elimination approach for visual sensor networks. Zhang et al. [2] studied relocation of sensors with minimum number of mobile sensors. The coding means [3–5] in network communication have been used. A fast motion estimation method is proposed to reduce the encoding complexity to 20% time saving [3]. For reducing the computational complexity, a content similarity based fast reference frame selection algorithm is also proposed [4]. Some optimal cluster-based mechanisms are proved to be efficient for load balancing with multiple mobile sinks for these problems [5].

However, Ahlswede et al. [6] originally proposed a new communication-efficient way over large-scale networks, i.e., network coding technology. Classical network coding (CNC) has been widely studied and

\* Corresponding author (email: yangyang7357@bjut.edu.cn)

it involves single-source multi-cast and  $k$ -pair uni-cast communication. CNC can solve perfectly the single-source multi-cast problem in the butterfly network.

Unfortunately, as a quantum counterpart of CNC, quantum network coding (QNC) for single-source multi-cast is impossible due to quantum no-cloning theorem [7] and thus it is reduced to the quantum  $k$ -pair uni-cast problem [8–16]. The demand for perfect QNC (fidelity 1) promoted the further study. Perfect QNC is infeasible without any additional quantum and classical resources [8–20], while QNC is feasible with fidelity no more than 0.983 in error-free quantum channels with capacity 1 without any additional resources. To overcome such imperfection and low transmission efficiency flaws, additional classical resources or pre-shared multi-particle quantum entanglement including local and global entanglement were introduced [9–20]. However, generally the preparation and coherence maintenance of prior multi-particle global entanglement is not easy especially in large-scale network. Up to now, only ten-photon quantum entanglement can be prepared using the present technique [21].

Although there are lots of studies on QNC, Leung et al. [22] pointed out that routing turns out optimal if an asymptotically large number of uses of the (quantum) butterfly network is allowable. This contrasts with the advantage of CNC, and demonstrates the difference between quantum and classical information. They also studied communication scenarios with various auxiliary resources and demonstrated that optimality of routing is essentially unchanged.

Quantum walks (QWs) [23] have received much attention for their intrinsic interest and many possible uses and they have been experimentally demonstrated [24–27]. Babatunde et al. [28] investigated the possibility of using a biased one-dimensional (1D) quantum walk to act as a router. Zhan et al. [29] showed that a perfect state transfer (PST) of an arbitrary unknown single-qubit state and that of an arbitrary unknown two-qubit state can be achieved through a 1D discrete-time QW on a line and a 2D discrete-time QW on a two-dimensional lattice, respectively. Yalçınkaya and Gedik [30] studied the perfect transfer of an unknown qubit state via the discrete-time QW on a line or a circle. Periodicity has been first discussed by Travaglione et al. [31] for the 4-cycle. They have shown the full-revival of the initial quantum state  $|\Phi_0\rangle = |\uparrow\rangle \otimes |0\rangle$  after 8 steps with a Hadamard coin. Later, Tregenna et al. [32] have extended this result by showing that, except the 7-cycle, all  $N$ -cycles with  $N < 11$  manifest periodicity with appropriate choices of the parameters  $(\rho, \theta, \varphi)$  for every initial coin state. These observations offer a new perspective to analyze the solvability for quantum multi-unicast network in a QW architecture. This QW architecture plays an important role in this paper for analyzing the specific multi-unicast network. However, this does not imply anything about the specific QW models on specific graphs (graph, conditional shift operator and coin flip operator) which need to be designed properly.

The purpose of this paper is twofold. We attempt to either propose a new approach to analyze the solvability over multi-unicast network or design constructive protocols with lower resources cost in a QW architecture. The coin states as the internal degree of freedom of two walkers represent the quantum states to be transferred. QW drives the transmission of the coin states from the source node to the sink via the butterfly network and the inverted crown network, respectively. By subtly constructing the cycle, the coin operator and the conditional shift operator, perfect state transmission can be achieved.

The rest of this paper is organized as follows. In Section 2, preliminaries are provided about the knowledge of discrete-time QW and graph. In Section 3, we analyze the solvability on 2-unicast session over the butterfly network, and design constructive protocols in a QW framework. In Section 4, we analyze the solvability on 3-unicast session over the inverted crown network, and design constructive protocols in a QW framework. In Section 5, we discuss the resource consumption and conclude this paper in Section 6.

## 2 Preliminaries

**Definition 1** (Graph). A undirected graph  $G$  includes a set of vertices  $V = \{v_1, v_2, v_3, \dots\}$  and edge set  $E = \{(v_i, v_j), (v_k, v_l), \dots\}$ , where  $E$  is a set of unordered pairs of connected vertices. If there are  $d$  edges incident on a vertex  $v_i$ , we say that  $v_i$  has degree  $d$ . A graph  $G$  with  $N$  vertices is described by its

adjacency matrix called  $Q$ , which is an  $N \times N$  matrix satisfying  $Q_{ij} = 1$  if  $(v_i, v_j) \in E$  otherwise it is zero. The adjacency matrix of the graph  $G$  contains all information about the graph so that it is unique to the topology of the graph.

**Definition 2** (Discrete-time quantum walk). The time evolution of the discrete-time quantum walk on a graph is controlled by the application of the unitary operator  $U = S(I \otimes C)$  where  $S$  is the conditional shift operator which affects both the coin space  $\mathcal{H}_c$  and the position space  $\mathcal{H}_p$ . Here  $\mathcal{H}_c$  and  $\mathcal{H}_p$  are spanned by the coin orthogonal basis  $\{|0\rangle, |1\rangle\}$  and the position states  $\{|x\rangle, x \in \mathbb{Z}\}$ , respectively.  $C$  is the coin operator which only affects the coin space  $\mathcal{H}_c$  and  $I$  is the identity operator applied on the position space  $\mathcal{H}_p$ .

For one-dimensional discrete-time QW on a line, the most general coin operator can be written as

$$C = \begin{bmatrix} \sqrt{\rho} & \sqrt{1-\rho}e^{i\theta} \\ \sqrt{1-\rho}e^{i\varphi} & -\sqrt{\rho}e^{i(\theta+\varphi)} \end{bmatrix}, \tag{1}$$

where  $\rho$  denotes the bias of the coin, i.e.,  $\rho$  and  $1 - \rho$  are the probabilities for moving left and right, respectively. Here,  $\theta$  and  $\varphi$  are the parameters defining the most general unitary operator. For  $\rho=1/2$  and  $\theta=\varphi=0$ , we obtain the unbiased Hadamard operator. For  $\rho=1$  and  $\theta + \varphi = \pi$ , we can obtain the identity operator  $I$ . The conditional shift operator  $S_l$  is given by

$$S_l = |0\rangle\langle 0| \otimes \sum_x |x+1\rangle\langle x| + |1\rangle\langle 1| \otimes \sum_x |x-1\rangle\langle x|, \tag{2}$$

where the sum is taken over all discrete positions in the position space  $\mathcal{H}_p$ .  $x$  stands for the position of the walker. The position of the walker is changed from  $x$  to  $x+1$  if the coin state is  $|0\rangle$ . Otherwise, the walker's position is changed from  $x$  to  $x - 1$ . The conditional shift operator  $S_l$  decides the direction in which the walker moves.

For one-dimensional discrete-time QW on a cycle with  $N$  nodes, the conditional shift operator  $S_c$  is expressed as follows:

$$S_c = \begin{cases} |0\rangle\langle 0| \otimes |v_{i+1}\rangle\langle v_i| + |1\rangle\langle 1| \otimes |v_N\rangle\langle v_i|, & \text{for } i = 1, \\ |0\rangle\langle 0| \otimes |v_1\rangle\langle v_i| + |1\rangle\langle 1| \otimes |v_{i-1}\rangle\langle v_i|, & \text{for } i = N, \\ |0\rangle\langle 0| \otimes |v_{i+1}\rangle\langle v_i| + |1\rangle\langle 1| \otimes |v_{i-1}\rangle\langle v_i|, & \text{for } i \neq 1, N, \end{cases} \tag{3}$$

where the position of the walker is changed from  $v_i$  to  $v_{i+1}(v_N)$  if the coin state is  $|0\rangle$  ( $|1\rangle$ ) for  $i=1$ . The position of the walker is changed from  $v_i$  to  $v_1(v_{i-1})$  if the coin state is  $|0\rangle$  ( $|1\rangle$ ) for  $i = N$ . Otherwise, the walker's position changes from  $v_i$  to  $v_{i+1}(v_{i-1})$  for other  $i$ .

**Definition 3** (Perfect state transfer via the network). Assume  $N$  arbitrary quantum inputs  $|\psi_{A_1}\rangle, |\psi_{A_2}\rangle, \dots, |\psi_{A_N}\rangle$  at the source nodes  $A_1, A_2, \dots, A_N$  are transferred to the sink nodes  $B_1, B_2, \dots, B_N$ , respectively. If the state fidelity  $F_{B_i} = |\langle \psi_{A_i} | \psi_{B_i} \rangle| = 1$  for all  $i \in \{1, 2, \dots, N\}$  can be obtained via the network transmission, the state transfer is called perfect state transfer.

### 3 Two-unicast communication over the butterfly network

As mentioned by Soeda et al. [33] and Li et al. [10], the two-unicast communication can be regarded as performing a distributed swap operation over the butterfly network, where two arbitrary quantum inputs  $|\psi_1\rangle$  and  $|\psi_2\rangle$  at the source nodes  $A_1$  and  $A_2$  are transferred to the sink nodes  $B_1$  and  $B_2$ , respectively (Figure 1). We can denote this as a distributed computation  $U_{\text{swap}}|\psi_1\rangle_{A_1}|\psi_2\rangle_{A_2} = |\psi_2\rangle_{B_2}|\psi_1\rangle_{B_1}$ . It can be shown that any unitary map on the photon creation operators can be decomposed into a non-interacting QW, and similarly any non-interacting QW can be expressed as such a unitary network [34]. In this paper, we show that the two qubit states  $|\psi_1\rangle$  and  $|\psi_2\rangle$  are transferred simultaneously from the source nodes  $A_1$  and  $A_2$  to the sink nodes  $B_1$  and  $B_2$ , respectively in a discrete-time QW architecture.

Every vertex of the graph  $G$  corresponds to a node in the butterfly network. The edges connecting these vertices specify the quantum channels between these nodes in the butterfly network in Figure 1(a). In this

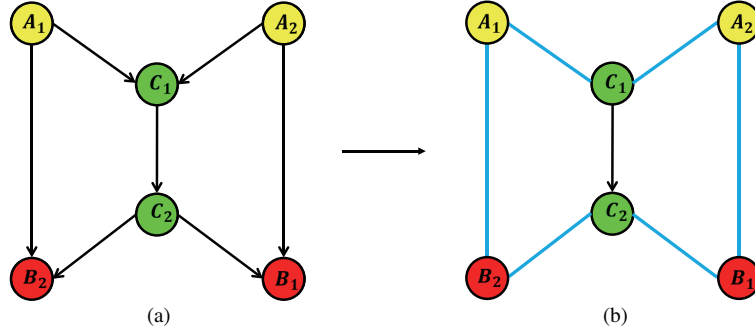


**Figure 1** (Color online) The butterfly network and its corresponding graph. (a) The butterfly network and (b) 6-cycle. The six nodes connected by blue lines consist of a 6-cycle.  $A_1$  and  $A_2$  are source nodes. Target nodes  $B_1$  and  $B_2$ , and intermediate nodes  $C_1$  and  $C_2$ .

proposed protocol, we assume that classical communication is free. As mentioned by Leung et al. [22], free classical communication can effectively reverse the direction of the quantum channels. Thus, free classical communication makes quantum networks undirected. Based on this conclusion, we describe new quantum network communication protocols for the butterfly network in a QW framework.

According to the calculations by Yalçınkaya and Gedik [30], PST can be achieved if  $A_1$  and  $B_1$  ( $A_2$  and  $B_2$ ) are the first and  $(\frac{N}{2} + 1)$ th sites for the  $N$ -cycle with even  $N$ . They showed that PST can be achieved via a discrete QW with various settings of parameters of coin operators on the  $N$ -cycle with even  $N$ . For example, the coin operator with  $\rho=1$  or identity operator allows PST on the  $N$ -cycle with even  $N$ . According to the conclusion of [30], we construct a 6-cycle in Figure 1(b).

Assume that two arbitrary quantum inputs to be transferred  $|\psi_1\rangle$  and  $|\psi_2\rangle$  are  $|\psi_1\rangle = \alpha_1 |0\rangle + \beta_1 |1\rangle$  and  $|\psi_2\rangle = \alpha_2 |0\rangle + \beta_2 |1\rangle$ , which are the initial coin states of the two walkers at the initial positions  $A_1$  and  $A_2$ , respectively, and satisfy the constraints:  $|\alpha_1|^2 + |\beta_1|^2 = 1$ ,  $|\alpha_2|^2 + |\beta_2|^2 = 1$ . The total input quantum states at the nodes  $A_1$  and  $A_2$  are  $|\varphi_1\rangle = |A_1\rangle \otimes |\psi_1\rangle$  and  $|\varphi_2\rangle = |A_2\rangle \otimes |\psi_2\rangle$ , respectively.  $|A_1\rangle$  and  $|A_2\rangle$  are the initial position states of the two walkers. The total quantum state of the two-walker QW is  $|\Phi_0\rangle = |\varphi_1\rangle \otimes |\varphi_2\rangle$ . The two-walker QW takes place in the Hilbert space  $\mathcal{H}_t = \mathcal{H}_1 \otimes \mathcal{H}_2$ , where  $\mathcal{H}_1 = \mathcal{H}_{p_1} \otimes \mathcal{H}_{c_1}$ , and  $\mathcal{H}_2 = \mathcal{H}_{p_2} \otimes \mathcal{H}_{c_2}$ . The mathematical representation after  $t$  steps can be given by

$$|\Phi_t\rangle = (S(I \otimes C))^t |\Phi_0\rangle, \quad (4)$$

where  $(S(I \otimes C))^t$  means that the  $S$  operation and the  $C$  operation are applied iteratively on  $|\Phi_0\rangle$  for  $t$  times.

$$S = \begin{cases} I \otimes S_2, & k = i \neq B_2, \\ S_1 \otimes I, & k = i \neq B_1, \\ S_1 \otimes S_2, & k \neq i, \end{cases} \quad (5)$$

where  $k = i$  represents both walkers are at the same node. Because of the capacity of quantum channels bounded by one, only a walker can move when the two walkers are at the same node.

$$S_1 = \begin{cases} |0\rangle\langle 0| (|C_1\rangle\langle A_1| + |A_2\rangle\langle C_1| + |B_1\rangle\langle A_2| + |C_2\rangle\langle B_1| + |B_2\rangle\langle C_2| + |A_1\rangle\langle B_2|) \\ \quad + |1\rangle\langle 1| (|B_2\rangle\langle A_1| + |A_1\rangle\langle C_1| + |C_1\rangle\langle A_2| + |A_2\rangle\langle B_1| + |B_1\rangle\langle C_2| + |C_2\rangle\langle B_2|), & i \neq B_1, \\ I, & i = B_1, \end{cases} \quad (6)$$

$$S_2 = \begin{cases} |0\rangle\langle 0| (|C_1\rangle\langle A_1| + |A_2\rangle\langle C_1| + |B_1\rangle\langle A_2| + |C_2\rangle\langle B_1| + |B_2\rangle\langle C_2| + |A_1\rangle\langle B_2|) \\ \quad + |1\rangle\langle 1| (|B_2\rangle\langle A_1| + |A_1\rangle\langle C_1| + |C_1\rangle\langle A_2| + |A_2\rangle\langle B_1| + |B_1\rangle\langle C_2| + |C_2\rangle\langle B_2|), & k \neq B_2, \\ I, & k = B_2, \end{cases} \quad (7)$$

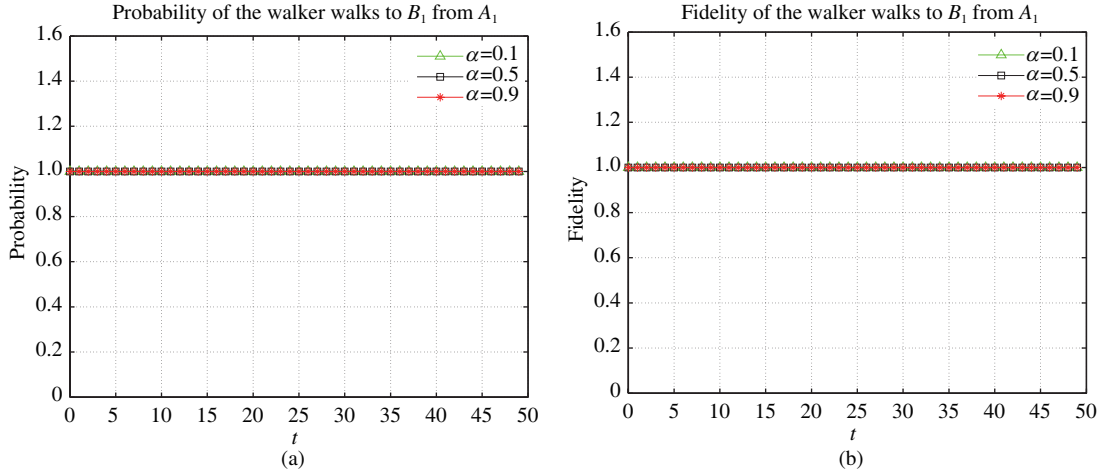


**Figure 2** (Color online) Probability (a) and fidelity (b) the QW from  $A_1$  to  $B_1$  at the butterfly network. The number of steps  $t = (N/2) + n \times N$ ,  $N = 6$ ,  $n = 0, 1, 2, 3, \dots$ , and  $\alpha$  is the amplitude of the initial coin state  $|\psi_0\rangle = \alpha|0\rangle + \beta|1\rangle$ .

The QW procedure can be implemented by repeatedly applying the coin operator  $C$  and conditional shift operator  $S$ , where  $C = C_1 \otimes C_2$ . We restrict the two coin operators of the two walkers to the identity operator  $I$ .

After  $t$  steps, the joint position probability of the walkers 1 and 2 located at nodes  $B_1$  and  $B_2$  respectively, is

$$P(B_1, B_2, t) = \sum_i \sum_j |\langle i, j, B_1, B_2 | \Phi_t \rangle|^2. \quad (8)$$

The reduced density matrices  $\rho_{p_1 c_1, t}$  and  $\rho_{p_2 c_2, t}$  can be obtained by tracing the density matrix  $\rho_t = |\Phi_t\rangle \langle \Phi_t|$  over subsystems  $p_2$  and  $c_2$ , and subsystems  $p_1$  and  $c_1$ , respectively.

$$\rho_{p_1 c_1, t} = \text{Tr}_{p_2 c_2}(\rho_t), \quad (9)$$

$$\rho_{p_2 c_2, t} = \text{Tr}_{p_1 c_1}(\rho_t). \quad (10)$$

The walkers 1 and 2 are initially localized at nodes  $A_1$  and  $A_2$ , respectively. We are interested in to what extent the walker 1(2)'s coin state is transferred from  $A_1$  to  $B_1$  (from  $A_2$  to  $B_2$ ). For this goal, we define the state fidelity at time  $t$  and node  $B_1$  ( $B_2$ ) by

$$F_{B_1, t} = \sqrt{\langle \Psi_{B_1} | \rho_{p_1 c_1, t} | \Psi_{B_1} \rangle}, \quad (11)$$

$$F_{B_2, t} = \sqrt{\langle \Psi_{B_2} | \rho_{p_2 c_2, t} | \Psi_{B_2} \rangle}, \quad (12)$$

where  $|\Psi_{B_1}\rangle = |B_1\rangle \otimes |\psi_1\rangle$ , and  $|\Psi_{B_2}\rangle = |B_2\rangle \otimes |\psi_2\rangle$ .  $\rho_{p_1 c_1, t}$  and  $\rho_{p_2 c_2, t}$  are the reduced density operators of the walkers 1 and 2 at time  $t$ .  $|\psi_1\rangle$  and  $|\psi_2\rangle$  are the transferred coin states at the nodes  $A_1$  and  $A_2$  for  $t=0$ , respectively. A PST occurs if  $F_{B_1, t} = 1$  and  $F_{B_2, t} = 1$ .

By applying iteratively the  $S$  operation and the  $C$  operation on  $|\Phi_0\rangle$ , the coin states  $|\psi_1\rangle$  and  $|\psi_2\rangle$  are transmitted from  $A_1$  to  $B_1$ , and  $A_2$  to  $B_2$  respectively at  $t = (N/2) + n \times N$ ,  $N = 6$ ,  $n = 0, 1, 2, 3, \dots$ . It is shown that the fidelity and the probability approach both 1 for arbitrary coin states. The numerical simulation results for the PST from  $A_1$  to  $B_1$  are shown in Figure 2.

#### 4 Three-unicast communication over the inverted crown network

In the inverted crown network, the source nodes are  $A_1$ ,  $A_2$  and  $A_3$ , respectively. They want to communicate with the target nodes  $B_1$ ,  $B_2$  and  $B_3$ , respectively.  $C_1$  and  $C_2$  are the intermediate nodes. The graph that all nodes are connected by edges looks like an inverted crown, as shown in Figure 3(a).

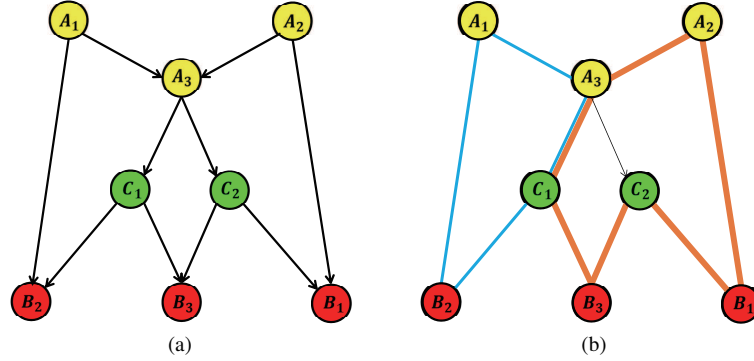


**Figure 3** (Color online) The inverted crown network and its corresponding graph. (a) The inverted crown network. (b) The corresponding graph.  $A_1, A_2$  and  $A_3$  are the source nodes. The target nodes are  $B_1, B_2$  and  $B_3$ , and the intermediate nodes are  $C_1$  and  $C_2$ . A cycle is composed of the edges with the same roughness.

The goal of the protocol is to transfer the coin states of  $A_1$  to  $B_1$ ,  $A_2$  to  $B_2$ , and  $A_3$  to  $B_3$ , simultaneously and individually. However, the inverted crown network consists of  $N = 8$  nodes. The pairs  $\{A_1, B_1\}$  and  $\{A_2, B_2\}$  cannot satisfy the constraint of PST: they should be the  $\{1\text{th}, (\frac{N}{2} + 1)\text{th}\}$  sites if they are chosen as the outermost sites on the  $N$ -cycle with even  $N$ . Although the pair  $\{A_3, B_3\}$  satisfies the condition of being the  $\{1\text{th}, (\frac{N}{2} + 1)\text{th}\}$  sites, it is possibly not optimal to transfer the state  $|\psi_3\rangle$  from  $A_3$  to  $B_3$  via a QW on 8-cycle. Therefore, to apply the conclusion on the PST on an  $N$ -cycle with even  $N$ , we design the efficient QW process to achieve the PST from  $A_1$  to  $B_1$ ,  $A_2$  to  $B_2$ , and  $A_3$  to  $B_3$ , respectively.

To achieve the PST from  $A_1$  to  $B_1$ , we divide the process into two sub-cycles as exhibited in Figure 3(b).

- $G_1 = \{A_1, A_3, C_1, B_2\}$ . By running the QW on the cycle  $G_1$ , the coin state  $|\psi_1\rangle$  is first transferred perfectly from  $A_1$  to  $C_1$ .

- $G_2 = \{C_1, A_3, A_2, B_1, C_1, B_3\}$ .  $C_1$  relays the coin state  $|\psi_1\rangle$  to  $B_1$  via the QW on the cycle  $G_2$ .

Due to the symmetry, to achieve the PST from  $A_2$  to  $B_2$ , we divide the process into two parts for the PST.

- $G_3 = \{A_2, A_3, C_2, B_1\}$ . By running the QW on the cycle  $G_3$ , the coin state  $|\psi_2\rangle$  is first transferred perfectly from  $A_2$  to  $C_2$ .

- $G_4 = \{C_2, A_3, A_1, B_2, C_1, B_3\}$ .  $C_2$  relays the coin state  $|\psi_2\rangle$  to  $B_2$  via the QW on the cycle  $G_4$ .

To achieve the PST from  $A_3$  to  $B_3$  efficiently, we design the graph as  $G_5 = \{A_3, C_1, B_3, C_2\}$ .

Assume that three arbitrary quantum inputs to be transferred  $|\psi_1\rangle, |\psi_2\rangle$ , and  $|\psi_3\rangle$  are  $|\psi_1\rangle = \alpha_1 |0\rangle + \beta_1 |1\rangle$ ,  $|\psi_2\rangle = \alpha_2 |0\rangle + \beta_2 |1\rangle$ , and  $|\psi_3\rangle = \alpha_3 |0\rangle + \beta_3 |1\rangle$  which are the initial coin states of the three walkers at the initial positions  $A_1, A_2$  and  $A_3$ , respectively, and satisfy the constraints:  $|\alpha_1|^2 + |\beta_1|^2 = 1$ ,  $|\alpha_2|^2 + |\beta_2|^2 = 1$ ,  $|\alpha_3|^2 + |\beta_3|^2 = 1$ . The total input quantum states at the nodes  $A_1, A_2$  and  $A_3$  are  $|\varphi_1\rangle = |A_1\rangle \otimes |\psi_1\rangle$ ,  $|\varphi_2\rangle = |A_2\rangle \otimes |\psi_2\rangle$  and  $|\varphi_3\rangle = |A_3\rangle \otimes |\psi_3\rangle$ , respectively.  $|A_1\rangle, |A_2\rangle$  and  $|A_3\rangle$  are the initial position states of the three walkers. The total quantum state of the three-walker QW is  $|\Psi_0\rangle = |\varphi_1\rangle \otimes |\varphi_2\rangle \otimes |\varphi_3\rangle$ .

The three-walker QW takes place in the Hilbert space  $\mathcal{H}_t = \mathcal{H}_1 \otimes \mathcal{H}_2 \otimes \mathcal{H}_3$ , where  $\mathcal{H}_1 = \mathcal{H}_{p_1} \otimes \mathcal{H}_{c_1}$ ,  $\mathcal{H}_2 = \mathcal{H}_{p_2} \otimes \mathcal{H}_{c_2}$  and  $\mathcal{H}_3 = \mathcal{H}_{p_3} \otimes \mathcal{H}_{c_3}$ .

The proposed protocol includes two phases and is described as follows.

**(1) The first phase: PST from  $A_1$  to  $C_1$ ,  $A_2$  to  $C_2$ , and  $A_3$  to  $B_3$ .**

The three walkers 1–3 take the walk on the graphs  $G_1, G_3$  and  $G_5$ , respectively. The mathematical representation after  $t_1$  steps can be given by

$$|\Psi_{t_1}\rangle = (S(I \otimes C))^{t_1} |\Psi_0\rangle, \quad (13)$$

where  $(S(I \otimes C))^{t_1}$  means that the  $S$  operation and the  $C$  operation are applied iteratively on  $|\Psi_0\rangle$  for

$t_1$  times.

$$S = \begin{cases} S_1 \otimes S_2 \otimes S_3, & i \neq j \neq k, \\ I \otimes S_2 \otimes S_3, & C_2 \neq i = j \neq k; B_3 \neq i = k \neq j, \\ S_1 \otimes S_2 \otimes I, & C_1 \neq i = k \neq j; C_2 \neq j = k \neq i, \\ I \otimes I \otimes S_3, & i = j = k \neq B_3, \\ I \otimes S_2 \otimes I, & i = j = k \neq C_2, \\ S_1 \otimes I \otimes I, & i = j = k \neq C_1, \\ S_1 \otimes I \otimes S_3, & B_3 \neq j = k \neq i; C_1 \neq i = j \neq k, \end{cases} \quad (14)$$

$$C = C_1 \otimes C_2 \otimes C_3 = I \otimes I \otimes I, \quad (15)$$

where  $i, j, k$  represent the nodes which the walkers 1–3 are at respectively. And  $i = j = k$  represents the three walkers are at the same node.

$$S_1 = \begin{cases} |0\rangle\langle 0| (|A_3\rangle\langle A_1| + |C_1\rangle\langle A_1| + |B_2\rangle\langle C_1| + |A_1\rangle\langle B_2|) \\ \quad + |1\rangle\langle 1| (|B_2\rangle\langle A_1| + |A_3\rangle\langle C_1| + |A_1\rangle\langle A_3| + |C_1\rangle\langle B_2|), & i \neq C_1, \\ I, & i = C_1, \end{cases} \quad (16)$$

$$S_2 = \begin{cases} |0\rangle\langle 0| (|B_1\rangle\langle A_2| + |A_2\rangle\langle A_3| + |A_3\rangle\langle C_2| + |C_2\rangle\langle B_1|) \\ \quad + |1\rangle\langle 1| (|A_3\rangle\langle A_2| + |B_1\rangle\langle C_2| + |C_2\rangle\langle A_3| + |A_2\rangle\langle B_1|), & j \neq C_2, \\ I, & j = C_2, \end{cases} \quad (17)$$

$$S_3 = \begin{cases} \{|0\rangle\langle 0| (|C_2\rangle\langle A_3| + |B_3\rangle\langle C_2| + |A_3\rangle\langle C_1| + |C_1\rangle\langle B_3|) \\ \quad + |1\rangle\langle 1| (|C_1\rangle\langle A_3| + |B_3\rangle\langle C_1| + |C_2\rangle\langle B_3| + |A_3\rangle\langle C_2|), & k \neq B_3, \\ I, & k = B_3. \end{cases} \quad (18)$$

The reduced density matrices  $\rho_{p_1c_1,t_1}$ ,  $\rho_{p_2c_2,t_1}$  and  $\rho_{p_3c_3,t_1}$  are the reduced density operators of the walkers 1–3 at time  $t_1$  and they can be obtained by tracing the density matrix  $\rho_{t_1} = |\Psi_{t_1}\rangle\langle\Psi_{t_1}|$  over the subsystems  $p_1$  and  $c_1$ ,  $p_2$  and  $c_2$ , and  $p_3$  and  $c_3$ , respectively.

$$\rho_{p_1c_1,t_1} = \text{Tr}_{p_2c_2;p_3c_3}(\rho_{t_1}), \quad (19)$$

$$\rho_{p_2c_2,t_1} = \text{Tr}_{p_1c_1;p_3c_3}(\rho_{t_1}), \quad (20)$$

$$\rho_{p_3c_3,t_1} = \text{Tr}_{p_1c_1;p_2c_2}(\rho_{t_1}). \quad (21)$$

The state fidelity at time  $t_1$  and the nodes  $C_1, C_2$ , and  $B_3$  are as follows:

$$F_{C_1,t_1} = \sqrt{\langle\Psi_{C_1}|\rho_{p_1c_1,t_1}|\Psi_{C_1}\rangle}, \quad (22)$$

$$F_{C_2,t_1} = \sqrt{\langle\Psi_{C_2}|\rho_{p_2c_2,t_1}|\Psi_{C_2}\rangle}, \quad (23)$$

$$F_{B_3,t_1} = \sqrt{\langle\Psi_{B_3}|\rho_{p_3c_3,t_1}|\Psi_{B_3}\rangle}, \quad (24)$$

where  $|\Psi_{C_1}\rangle = |C_1\rangle \otimes |\psi_1\rangle$ ,  $|\Psi_{C_2}\rangle = |C_2\rangle \otimes |\psi_2\rangle$ , and  $|\Psi_{B_3}\rangle = |B_3\rangle \otimes |\psi_3\rangle$ . The formulas  $F_{C_1,t_1} = 1$ ,  $F_{C_2,t_1} = 1$ , and  $F_{B_3,t_1} = 1$  hold. This is because the pairs  $\{A_1, B_1\}$  and  $\{A_2, B_2\}$  can satisfy the constraint of PST: they are the {1st, 3th} sites if they are chosen as the outermost sites on the cycles  $G_1, G_3$  and  $G_5$ , respectively.

**(2) The second phase: PST from  $C_1$  to  $B_1$ , and  $C_2$  to  $B_2$ .**

Since the PST has been done from  $A_3$  to  $B_3$ , in this phase only the PST from  $C_1$  to  $B_1$ , and  $C_2$  to  $B_2$  is considered.



In this phase, the two walkers 1 and 2 take the walk on the graphs  $G_2$  and  $G_4$ , respectively. The total quantum states at the nodes  $C_1$  and  $C_2$  are  $|\varphi'_1\rangle = |C_1\rangle \otimes |\psi_1\rangle$ ,  $|\varphi'_2\rangle = |C_2\rangle \otimes |\psi_2\rangle$ , respectively. The total quantum state of the two-walker QW is  $|\Psi'_0\rangle = |\varphi'_1\rangle \otimes |\varphi'_2\rangle$ .

The mathematical representation after  $t_2$  steps can be given by

$$|\Psi_{t_2}\rangle = (S'(I \otimes C))^{t_2} |\Psi'_0\rangle, \quad (25)$$

where

$$S' = \begin{cases} I \otimes S'_2, & i = j \neq B_2, \\ S'_1 \otimes I, & i = j \neq B_1, \\ S'_1 \otimes S'_2, & i \neq j, \end{cases} \quad (26)$$

$$C = C_1 \otimes C_2 = I \otimes I, \quad (27)$$

where  $i, j$  represent the nodes which the walkers 1 and 2 are at respectively. And  $i = j$  represents the two walkers are at the same node.

$$S'_1 = \begin{cases} |0\rangle\langle 0| (|A_3\rangle\langle C_1| + |A_2\rangle\langle A_3| + |B_1\rangle\langle A_2| + |C_2\rangle\langle B_1| + |B_3\rangle\langle C_2| + |C_1\rangle\langle B_3|) \\ \quad + |1\rangle\langle 1| (|B_3\rangle\langle C_1| + |C_2\rangle\langle B_3| + |B_1\rangle\langle C_2| + |A_2\rangle\langle B_1| + |A_3\rangle\langle A_2| + |C_1\rangle\langle A_3|), & i \neq B_1, \\ I, & i = B_1, \end{cases} \quad (28)$$

$$S'_2 = \begin{cases} |0\rangle\langle 0| (|B_3\rangle\langle C_2| + |C_1\rangle\langle B_3| + |B_2\rangle\langle C_1| + |A_1\rangle\langle B_2| + |A_3\rangle\langle A_1| + |C_2\rangle\langle A_3|) \\ \quad + |1\rangle\langle 1| (|A_3\rangle\langle C_2| + |A_1\rangle\langle A_3| + |B_2\rangle\langle A_1| + |C_1\rangle\langle B_2| + |B_3\rangle\langle C_1| + |C_2\rangle\langle B_3|), & j \neq B_2, \\ I, & j = B_2. \end{cases} \quad (29)$$

The reduced density matrices  $\rho_{p_1 c_1, t_2}$ ,  $\rho_{p_2 c_2, t_2}$  are the reduced density operators of the walkers 1 and 2 after  $t_2$  steps and they can be obtained by tracing the density matrix  $\rho_{t_2} = |\Psi_{t_2}\rangle\langle\Psi_{t_2}|$  over the subsystems  $p_2$  and  $c_2$ ,  $p_1$  and  $c_1$ , respectively.

$$\rho_{p_1 c_1, t_2} = \text{Tr}_{p_2 c_2}(\rho_{t_2}), \quad (30)$$

$$\rho_{p_2 c_2, t_2} = \text{Tr}_{p_1 c_1}(\rho_{t_2}). \quad (31)$$

The state fidelity at time  $t_2$  and the nodes  $B_1, B_2$  are as follows:

$$F_{B_1, t_2} = \sqrt{\langle\Psi_{B_1}|\rho_{p_1 c_1, t_2}|\Psi_{B_1}\rangle}, \quad (32)$$

$$F_{B_2, t_2} = \sqrt{\langle\Psi_{B_2}|\rho_{p_2 c_2, t_2}|\Psi_{B_2}\rangle}, \quad (33)$$

where  $|\Psi_{B_1}\rangle = |B_1\rangle \otimes |\psi_1\rangle$  and  $|\Psi_{B_2}\rangle = |B_2\rangle \otimes |\psi_2\rangle$ . The formulas  $F_{B_1, t_2} = 1$  and  $F_{B_2, t_2} = 1$  hold. This is because the pairs  $\{C_1, B_1\}$  and  $\{C_2, B_2\}$  can satisfy the constraint of PST: they are the {1st, 4th} sites if they are chosen as the outermost sites on the cycles  $G_2$  and  $G_4$ , respectively.

To summarize, the coin states  $|\psi_1\rangle, |\psi_2\rangle$  and  $|\psi_3\rangle$  can be transferred from  $A_1$  to  $B_1$ ,  $A_2$  to  $B_2$ ,  $A_3$  to  $B_3$  respectively with both probability and fidelity 1.

## 5 Discussion

Resource consumption is an important indicator of evaluating a QNC protocol. Firstly, we compared our scheme with existing QNC protocols in terms of prior local or global entanglement, classical communication and necessary quantum operation, as shown in Table 1.

In [35], Raussendorf et al. introduced another metric of the resource consumption, i.e., three parameters: spatial resources  $S$ , operational resources  $O$  and temporal resources  $T$ . Spatial resources  $S$  can be defined as the number of the required particles associated to a given network  $G$ . The operational



**Table 1** Comparison in terms of resource consumption and fidelity

	Prior entanglement	Classical communication	Quantum operation	Average fidelity	Probability
Ref. [3]	Yes	Yes	Yes	$0.5 \leq f \leq 1$	1
Refs. [4, 6, 9–14]	Yes	Yes	Yes	1	1
Refs. [5, 15]	Yes	Yes	Yes	1	$p \leq 1$
Our scheme	No	Yes	Yes	1	1

resources  $O$  can be defined as the total number of quantum unitary operations involved. As for the temporal resources, specified by the logical depth  $T$  is the minimum number of quantum unitary operation rounds. In this paper, the spatial resource consumption is 2 in that only two walkers are used for the butterfly network and three walkers for the inverted crown network. Therefore, the spatial resource independent of the network size is always a constant. The probability and fidelity approach 1. Since the  $S$  operation and the  $C$  operation are applied iteratively on the position space and the coin space, the corresponding temporal resource consumption is also 2 in the butterfly network and 5 in the inverted crown network.

In conclusion, no prior local or global entanglement is necessary in our QW-based quantum multi-unicast communication protocol. Moreover, the spatial resource consumption is a constant independent of the network size in that only two walkers are used in the butterfly network and three walkers are used in the inverted crown network. The operational resource consumption is equivalent to the corresponding temporal resource consumption.

## 6 Conclusion

In summary, by introducing quantum walks into quantum network communication, we presented a quantum multi-unicast communication scheme over the butterfly network and the inverted crown network, respectively. In fact, our techniques can be applied to a more general graph. It paves a way to combine quantum computation and quantum network communication.

**Acknowledgements** This work was supported by National Natural Science Foundation of China (Grant Nos. 61572053, 61671087, U1636106, 61602019, 61472048, 61402148), Beijing Natural Science Foundation (Grant No. 4162005), and Natural Science Foundation of Hebei Province (Grant No. F2015205114).

## References

- Zhou Z L, Wu Q J, Huang F, et al. Fast and accurate near-duplicate image elimination for visual sensor networks. *Int J Distrib Sens N*, doi: 10.1177/1550147717694172
- Zhang Y H, Sun X M, Wang B W. Efficient algorithm for K-Barrier coverage based on integer linear programming. *China Commun*, 2016, 13: 16–23
- Pan Z Q, Lei J J, Zhang Y, et al. Fast motion estimation based on content property for low-complexity H. HEVC encoder. *IEEE Trans Broadcast*, 2016, 62: 675–684
- Pan Z Q, Jin P, Lei J J, et al. Fast reference frame selection based on content similarity for low complexity HEVC encoder. *J Vis Commun Image R*, 2016, 40: 516–524
- Zhang J, Tang J, Wang T B, et al. Energy-efficient data-gathering rendezvous algorithms with mobile sinks for wireless sensor networks. *Int J Sens Netw*, 2017, 23: 248–257
- Ahlswede R, Cai N, Li S-Y R, et al. Network information flow. *IEEE Trans Inf Theory*, 2000, 46: 1204–1216
- Wootters W K, Zurek W H. A single quantum cannot be cloned. *Nature*, 1982, 299: 802–803
- Hayashi M, Iwama K, Nishimura H, et al. Quantum network coding. In: *Proceedings of Annual Symposium on Theoretical Aspects of Computer Science*. Berlin: Springer, 2007. 4393: 610–621
- Hayashi M. Prior entanglement between senders enables perfect quantum network coding with modification. *Phys Rev A*, 2007, 76: 040301
- Satoh T, Le Gall F, Imai H. Quantum network coding for quantum repeaters. *Phys Rev A*, 2012, 86: 032331
- Soeda A, Kinjo Y, Turner P S, et al. Quantum computation over the butterfly network. *Phys Rev A*, 2011, 84: 012333
- Li J, Chen X B, Xu G, et al. Perfect quantum network coding independent of classical network solutions. *IEEE Commun Lett*, 2015, 19: 115–118
- Li J, Chen X B, Sun X M, et al. Quantum network coding for multi-unicast problem based on 2D and 3D cluster states. *Sci China Inf Sci*, 2016, 59: 042301

- 14 Mahdian M, Bayramzadeh R. Perfect K-pair quantum network coding using superconducting qubits. *J Supercond Nov Magn*, 2015, 28: 345–348
- 15 Shang T, Li J, Pei Z, et al. Quantum network coding for general repeater networks. *Quantum Inf Process*, 2015, 14: 3533–3552
- 16 Xu G, Chen X-B, Li J, et al. Network coding for quantum cooperative multicast. *Quantum Inf Process*, 2015, 14: 4297–4322
- 17 Shang T, Du G, Liu J-W. Opportunistic quantum network coding based on quantum teleportation. *Quantum Inf Process*, 2016, 15: 1743–1763
- 18 Kobayashi H, Le Gall F, Nishimura H, et al. Perfect quantum network communication protocol based on classical network coding. In: *Proceedings of IEEE International Symposium on Information Theory (ISIT)*, Austin, 2010. 2686–2690
- 19 Kobayashi H, Le Gall F, Nishimura H, et al. Constructing quantum network coding schemes from classical nonlinear protocols. In: *Proceedings of IEEE International Symposium on Information Theory (ISIT)*, St. Petersburg, 2011. 109–113
- 20 Jain A, Franceschetti M, Meyer D A. On quantum network coding. *J Math Phys*, 2011, 52: 032201
- 21 Wang X-L, Chen L-K, Li W, et al. Experimental ten-photon entanglement. *Phys Rev Lett*, 2016, 117: 210502
- 22 Leung D, Oppenheim J, Winter A. Quantum network communication: the butterfly and beyond. *IEEE Trans Inf Theory*, 2010, 56: 3478–3490
- 23 Aharonov D, Ambainis A, Kempe J, et al. Quantum walks on graphs. In: *Proceedings of the 33rd ACM Symposium on Theory of Computing*, Hersonissos, 2001. 50–59
- 24 Ambainis A. Quantum walk algorithm for element distinctness. *SIAM J Comput*, 2007, 37: 210–239
- 25 Magniez F, Santha M, Szegedy M. Quantum algorithms for the triangle problem. *SIAM J Comput*, 2007, 37: 413–424
- 26 Tamascelli D, Zanetti L. A quantum-walk-inspired adiabatic algorithm for solving graph isomorphism problems. *J Phys A-Math Theor*, 2014, 47: 325302
- 27 Childs A M, Ge Y M. Spatial search by continuous-time quantum walks on crystal lattices. *Phys Rev A*, 2014, 89: 052337
- 28 Babatunde A M, Cresser J, Twamley J. Using a biased quantum random walk as a quantum lumped element router. *Phys Rev A*, 2014, 90: 012339
- 29 Zhan X, Qin H, Bian Z-H, et al. Perfect state transfer and efficient quantum routing: a discrete-time quantum-walk approach. *Phys Rev A*, 2014, 90: 012331
- 30 Yalçınkaya İ, Gedik Z. Qubit state transfer via discrete-time quantum walks. *J Phys A-Math Theor*, 2015, 48: 225302
- 31 Travaglione B C, Milburn G J. Implementing the quantum random walk. *Phys Rev A*, 2002, 65: 032310
- 32 Tregenna B, Flanagan W, Maile R, et al. Controlling discrete quantum walks: coins and initial states. *New J Phys*, 2003, 5: 83
- 33 Soeda A, Kinjo Y, Turner P S, et al. Quantum computation over the butterfly network. 2011. arXiv: 1010.4350v3
- 34 Rohde P P, Schreiber A, Stefanak M, et al. Increasing the dimensionality of quantum walks using multiple walkers. *J Comput Theor Nano*, 2013, 10: 1644–1652
- 35 Raussendorf R, Browne D E, Briegel H J. Measurement-based quantum computation on cluster states. *Phys Rev A*, 2003, 68: 022312